Article ID: 1000-324X(2012)07-0780-05 **DOI:** 10.3724/SP.J.1077.2011.12049

Investigation on Intercalation Modification of Sodium-montmorillonite by Cationic Surfactant

LIU Hua-Bin, XIAO Han-Ning

(College of Materials Science and Engineering, Hunan University, Changsha 410082, China)

Abstract: Sodium-montmorillonite (Na^+-MMT) was intercalation modified with octadecyl trimethyl ammonium chloride (OTAC) in aqueous suspension *via* an ion exchange mechanism. Fourier transform infrared spectroscopy (FTIR) study indicates that OTAC is successfully intercalated into Na^+-MMT layers and/or adsorbed on the surface of Na^+-MMT. X-ray diffraction (XRD) analysis revealed that the interlayer spacing of the Na^+-MMT was extended with the content of OTAC increasing, and the maximum spacing can reach about 3.80 nm. Results of scanning electron microscopy (SEM) analysis reveals the morphologies change from soherical-like particles to high-aspect ratio flakes after modification. Different configurations of OTA^+ chains within MMT interlayer are proposed based on the above analysis. The results of contact angle and the dispersion analysis show that the surface wettability of Na^+-MMT is converted from hydrophilic to organophilic.

Key words: montmorillonite; intercalation modification; microstructure; surface property; nanomaterials

Montmorillonite (MMT), one of the 2:1 layered silicates, has been widely used as adsorbent for industrial effluent treatment or for potable water treatment[1-3], due to its unique combination of interesting properties: high surface area, huge cation exchange capacity, good surface activity and low cost. MMT has also found its wide application in nanocomposites as inorganic fillers because of its typical well-layered structure. Polymeric nanocomposites consisting of a small amount of MMT not only can remarkably improve mechanical properties by strong interaction inside nanocomposite components[4-7], but also can offer some functional properties of the composites. For example, thermal stabilities can be improved by using MMT as a superior insulator and heat and mass transport barriers to the volatile products generated during decomposition[8-12]. Flame retardance can be realized by forming a high-performace carbonaceous-silicate char during burning[11,13-14]. Gas barrier performance of the nanocomposites can be enhanced by creating a maze or 'tortuous path' that retards the progress of the gas molecules through the matrix resin[15-17].

However the application effects greatly depend on the compatibility between the MMT fillers and polymer matrix and the status whether the former could be homogeneously dispersed in the latter one. The raw MMT has a strong hydrophilic surface and contains plenty of water inside the interlayer, which decreases the interface compatibility with organic resin. Beside, there is a serious aggregation in the raw MMT, which greatly influences the surface activity and its dispersibility in polymeric matrix. Surface modification is thus required to change the structural characteristics of MMT and further improve the interface compatibility. There are many studies reporting structural features of MMT clays before and after modification. Not limited to structure analysis, this work further focuses on the surface properties of the MMT clay modified by using cationic surfactant.

1 Experimental

1.1 Materials

The sodium-montmorillonite (Na^+-MMT) was provided by Fenghong Co., Ltd. (Zhejiang, China) with a cation exchange capacity (CEC) of 90 mmol/100 g. A quaternary surfactant, octadecyl trimethyl ammonium chloride (OTAC), was purchased from Tianjin Damao chemical corporation and used without further purification. Chemical grade hydrochloric acid (HCl) was added into MMT suspension, and analytical grade silver nitrate ($AgNO_3$) was used to detect the residual Cl ions. Deionized water was used throughout this work. Analytical grade toluene was used as the organic dispersion medium.

1.2 Modification of Na^+-MMT

The Na^+-MMT was modified according to a standard ion exchange procedure[18]. 10.0 g Na^+-MMT was dis-

Received date: 2012-01-30; **Modified date:** 2012-03-19; **Published online:** 2012-04-10
Foundation item: National Natural Science Foundation of China (50972042)
Biography: LIU Hua-Bin(1978–), candidate of PhD. E-mail: huabinliu@163.com
Corresponding author: XIAO Han-Ning, Professor. E-mail: hnxiao@hnu.edu.cn

persed in 500 mL of hot water at 70℃ under continuous stirring to obtain a suspension solution. A certain amount of OTAC and concentrated hydrochloric acid were dissolved in 200 mL of hot water at 70℃, and the resultant solution was poured into the MMT suspension solution under vigorous stirring for about 1.5 h. The content of OTAC added in terms of aqueous solution was changed between 0.2 CEC and 2.3 CEC in 0.3 CEC steps. After modification the reaction mixture solution was filtered and washed three times with hot water at 70℃ to remove un-adsorbed surfactant (until no precipitate was detected by 0.1 mol/L $AgNO_3$), after then washed twice with ethanol. The prepared organo-montmorillonite (OMMT) was dried finally in a vacuum oven at 70℃ for 36 h.

1.3 Characterization

Fourier transform infrared spectroscopy (FTIR) was carried out in a Nicolet-520 spectrometer to characterize the interface of OMMT (the OMMT was crushed and blended with potassium bromide (KBr)). X-ray diffraction (XRD) patterns of MMT and OMMT were collected on a Rigaku D/Max-2550 PC diffractometer using Cu Kα (λ=0.15406 nm) radiation in 2θ range 2–10° with 0.02°/s. The basal spacing was calculated according to Bragg law[19]. The morphology of Na^+-MMT and OMMT was observed by scanning electron microscopy (SEM, FEI NOVA200 Nanolab). The MMT powders were pressed into a flat sheet, and the contact angle was measured with water drop by a contact angle analyzer (Powereach JC2000C1).

Dispersion of OMMT samples in the purified liquids were prepared in a dry box. Amounts of 5–6 g OMMT were dispersed in toluene and shaken to get a homogeneous dispersion. The sediment volume of dispersions of 0.35 g OMMT in 35 mL toluene was measured in 50 mL graduated test tubes. After intense shaking, the sediment volume was measured after 24 h.

2 Results and discussion

2.1 Structure and morphology analysis of the OMMT

The FTIR spectra of Na^+-MMT before and after modification are shown in Fig. 1. Before modification (Fig. 1(a)) the band at 3610 cm^{-1} is assigned to the stretching vibrations of the –OH groups bonded to the aluminum and/or silicon in the Na^+-MMT interlayer. The broad band at 3460 cm^{-1} is assigned to the hydroxyl stretching vibrations, and the band at 1650 cm^{-1} corresponded to H–O–H bending vibrations shows the presence of some moisture in the samples.

While for the samples after modification (as shown in Fig. 1(b)) the stretching band of the –OH group at 3610 cm^{-1} was shifted to 3620 cm^{-1}, and this slight shift towards the smaller frequencies implies the removal of some structural hydroxyl groups from the Si–OH or Al–OH sites. The broad band at 3460 cm^{-1} in Fig. 1(a) was shifted to 3430 cm^{-1}. The new appearing bands at 2920 and 2850 cm^{-1} are attributed to asymmetric and symmetric C–H stretching vibrations of OTAC. The weak band at 3267 cm^{-1} is attributed to N–H stretching vibrations present in OTAC[20] and the peak at 1470 cm^{-1} is attributed to the CH_3–N^+ moiety. The adsorption strength difference of the reflections was observed with increasing C_{OTAC} (in Fig. 1(b) and (c)) implying the different exchange efficiency of the MMT clays.

Besides, the bands is in the range of 1300–400 cm^{-1} attributed to stretching and bending vibrations of Si–O–Al, Si–O–Si, and Al–O groups of all the samples have no obvious changes, which suggests that the main bones of Na^+-MMT clay before and after modification are similar and there were no other interactions except the ion exchange during the modification.

The XRD patterns of the Na^+-MMT and the OMMT are displayed in Fig. 2. After the OTAC modification, the peak at 2θ = 5.84° (corresponding to a basal plane spacing (d_{001}) of 1.51 nm for Na^+-MMT) was shifted to lower 2θ value. There is a weak reflection at 2θ of 5.72° (corresponding to a basal spacing (d_{001}) of 1.61 nm) for OMMT when C_{OTAC} is 0.2 CEC. The OMMT has two characteristic peaks at 2θ of 4.92° and 3.38° in case of C_{OTAC} = 0.5 CEC, corresponding to d_{001} values of 1.79 nm and 2.61 nm, respectively. Further increase of C_{OTAC} to 1.1 CEC, the characteristic peak of the OMMT moved to 3.68°, corresponding to d_{001} = 2.40 nm. When the C_{OTAC} increases to 1.7 CEC, the OMMT has an intense peak at 2θ = 2.85° corresponding to a basal plane spacing of 3.09 nm. The maximum

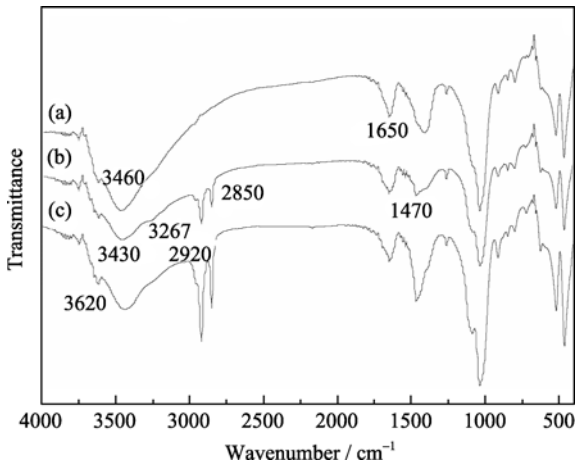

Fig. 1　FTIR spectra of Na^+-MMT before (a) and after modification ((b) and (c), at C_{OTAC} = 0.5 CEC and 2.0 CEC, respectively)

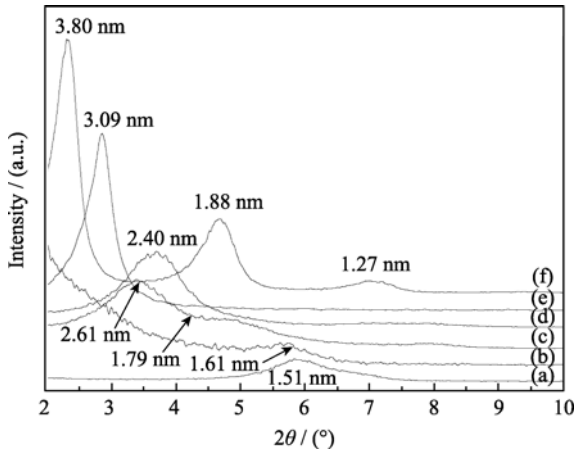

Fig. 2 XRD patterns of Na^+-MMT before (a) and after modification ((b)–(f): C_{OTAC} = 0.2 CEC (b); 0.5 CEC (c); 1.1 CEC (d) ; 1.7 CEC (e); 2.3 CEC(f))

interlayer spacing of OMMT reaches 3.80 nm at C_{OTAC} = 2.3 CEC. It is thus concluded that the interlayer spacing of the Na^+-MMT is extended by the intercalation modification. The peak at about 6.94° (1.27 nm in Fig. 2(f)) is attributed to the aggregation of the surfactant in the OMMT galleries[21].

Both the results of FTIR and XRD analysis indicate that the surfactants have been successfully intercalated into Na^+-MMT layers. It is known that the shape of a perfectly straight chain of OTA^+ looks like a 'nail', where the long alkyl chain is the 'nail-body' and the chain end holding three methyls is the 'nail-head'. The length of the nail is about 2.79 nm, consisting of the 'nail-head' (0.43 nm) and 'nail-body' (2.36 nm). The height of the 'nail-body' is about 0.46 nm and that of the 'nail-head' is about 0.51 nm, and the heights of the 'nail-body' and 'nail-head' are 0.41 nm and 0.67 nm, respectively, when the plane of the zigzag arrangement of the carbon atoms of OTA^+ is parallel to the plane of the MMT layer[18,22]. The thickness of a single MMT's TOT layer is about 0.96 nm[22-23]. The schematically illustration of five different configurations of OTC^+ chains in OMMT interlayer was proposed (as shown in Fig. 3) based on the results of the XRD analysis. The values of 1.61 nm and 1.79 nm for the OMMT are consistent with a monolayer arrangement of OTC^+ chains in the interlayer space (see Fig. 3(b)). The basal spacing of 1.88 nm for the OMMT is in agreement with a bilayer arrangement of OTC^+ chains in the interlayer space (see Fig. 3(c)). The basal spacings of 2.40 nm to 3.09 nm for the OMMT, corresponds to a pseudo trilayer to paraffin-type monolayer arrangement of intercalated OTC^+ chains (see Fig. 3(d) and (e)). The OTC^+ chains were thought to radiate away from the MMT layers forming bimolecular arrangement (see Fig. 3(f)).

The SEM results show the change of the morphology of Na^+-MMT clay before and after modification with OTAC. Before modification the Na^+-MMT was initially adhesive and aggregated to form a rather compact structure (shown in Fig. 4(a) and (b)). The irregular particle in different sizes was observed, and the bulk is nearly tens of micrometers. After modification the large particles were split into small ones because of the intercalation reaction with OTAC, and the compact structure got looser with curly margins (shown in Fig. 4(c) and (d)). The intercalation effect was enhanced with the C_{OTAC} increasing, the agglomeration was broken and the layers were further apart and less compact, displaying a leaf like structure (shown in Fig. 4(e) and (f)). The almost exfoliated layers were achieved at C_{OTAC}=2.0 CEC (shown in Fig. 4(g) and (h)). The significant variations of the morphologies observed by SEM are consistent with the findings of FTIR and XRD analysis.

2.2 Surface wettability of the OMMT

The contact angle was used to characterize the surface wettability. If the contact angle is less than 90°, the surface is described as hydrophilic; otherwise the surface is described as organophilic. The values of contact angle of MMT clay before and after modification were summarized in Table 1.

It is difficult to take an image of the water drop dropped on the Na^+-MMT before modification, which indicates the surface has strong hydrophilicity before modification. After modification the contact angle value increases with the C_{OTAC} increasing, which implies that the surface characteristic was converted from hydrophilic to organophilic. According to the principle of polarity compatibility, the dispersion effect will be improved when surface polarity of

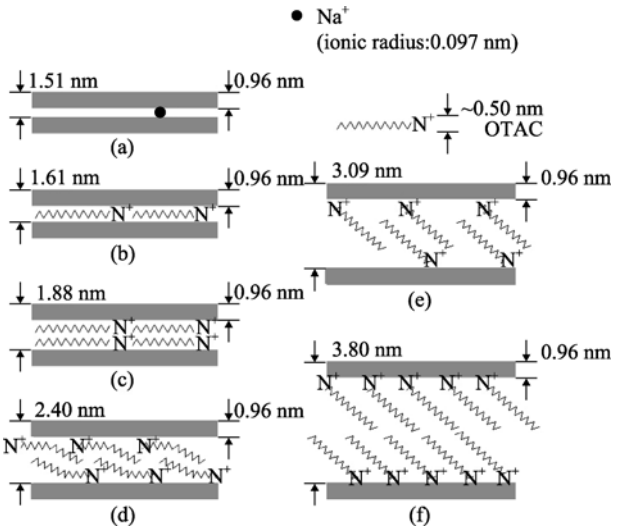

Fig. 3 Schematic illustration of five different arrangements of OTC^+ chains in OMMT interlayer

(a) Na^+-MMT; (b) Lateral monolayers; (c) Lateral bilayers; (d) Pseudotrimolecular layers of chains lying on the surface; (e) Paraffin-type monolayers; (f) Paraffin-type bialayers

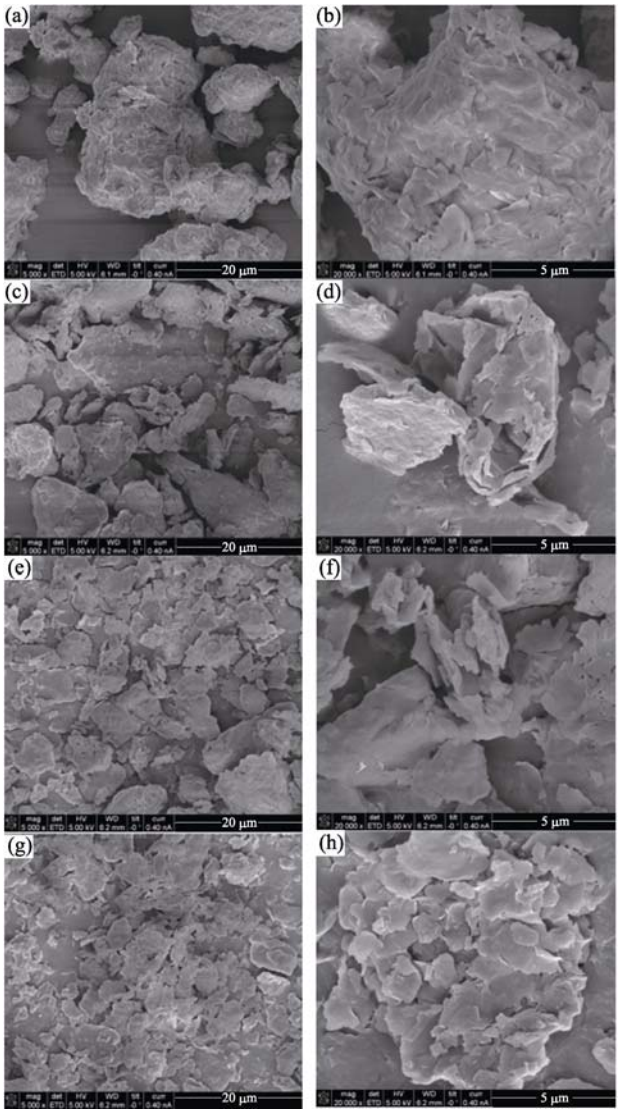

Fig. 4　SEM images of Na^+-MMT (a and b) and OMMT (c-h): C_{OTAC}=0.5 CEC ((c) and (d)), 1.4 CEC ((e) and (f)), 2.0 CEC ((g) and (h))

particles is similar to that of liquid media. Table 1 also displays the sediment volume in toluene after 24 h.

The sediment volume steeply decreases with the C_{OTAC} increasing. Before modification, the Na^+-MMT particles has a worse dispersibility and can not swell in toluene, and the supernatant is clear. While the OMMT particles has a better dispersibility and swell in toluene, and the supernatant is cloudy. The dispersion forms gels in case of $C_{OTAC} \geqslant 2.0$ CEC. The result shows that OMMT has a high affinity to organic medium.

Table 1　The variations of the contact angle of MMTs to water and the sediment volume of MMTs in toluene after 24 h

C_{OTAC} (*CEC)	Contact angle/(º)	Sediment volume /($cm^3 \cdot g^{-1}$)	Wettability
0	—	63.2	Hydrophilic
0.2	25	54.4	Hydrophilic
0.5	38	41.6	Weak Hydrophilic
0.8	49	22.3	Weak Hydrophilic
1.1	75	8.5	Nearly Neutral
1.4	82	3.0	Nearly Neutral
1.7	91	1.5	Organophilic
2.0	97	(gel)	Organophilic
2.3	113	(gel)	Organophilic

3　Conclusion

The Na^+-MMT was successfully intercalation modified by OTAC. Both the structure characteristics and surface properties of the layered clay changed after modification. The modified MMT clays with flake structure would show good compatibility with polymer matrix. The interlayer spacing of OMMT was extended from 1.51 nm to 3.80 nm, and the large particle with compact aggregation was exfoliated. The surface wettability of Na^+-MMT was converted from hydrophilic to organophilic after modification. Based on the analytical results, it is suggested that OTAC can be used to improve the performance of the MMT nanocomposites.

References:

[1] Xi Y, Ding Z, He H, *et al*. Structure of organoclays—an X-ray diffraction and thermogravimetric analysis study. *J. Colloid. Interface Sci.*, 2004, **277(1):** 116–120.

[2] Kim C S, Yates D M, Heaney P J. The layered sodium silicate magadiite: an analog to smectite for benzene sorption from water. *Clays Clay Miner.*, 1997, **45(6):** 881–885.

[3] Meincke O, Hoffmann B, Dietrich C, *et al*. Viscoelastic properties of polystyrene nanocomposites based on layered silicates. *Macromol. Chem. Phys.*, 2003, **204(5/6):** 823–830.

[4] Tabsan N, Wirasate S, Suchiva K. Abrasion behavior of layered silicate reinforced natural rubber. *Wear*, 2010, **269(5/6):** 394–404.

[5] Kawasumi M, Hasegawa N, Usuki A, *et al*. Nematic liquid crystal/clay mineral composites. *Mater. Sci. Eng., C*, 1998, **6(2/3):** 135–143.

[6] Vaia R A, Price G, Ruth P N, *et al*. Polymer/layered silicate nanocomposites as high performance ablative materials. *Appl. Clay Sci.*, 1999, **15(1/2):** 67–92.

[7] Wen J, Yin P, Zhen M. Friction and wear properties of UHMWPE/nano-MMT composites under oilfield sewage condition. *Mater. Lett.*, 2008, **62(25):** 4161–4163.

[8] Zanetti M, Camino G, Thomann R, *et al*. Synthesis and thermal behavior of layered silicate-EVA nanocomposites. *Polymer*, 2001, **42(10):** 4501–4507.

[9] Lim S T, Hyun Y H, Choi H J, *et al*. Synthetic biodegradable aliphatic polyester/montmorillonite nanocomposites. *Chem. Mater.*, 2002, **14(4):** 1839−1844.

[10] Alexandre M, Dubois P. Polymer-layered silicate nanocomposites: preparation, properties and uses of a new class of materials. *Mater. Sci. Eng.*, 2000, **28(1/2):** 1−63.

[11] Gilman J W. Flammability and thermal stability studies of polymer-layered silicate (clay) nanocomposites. *Appl. Clay Sci.*, 1999, **15(1/2):** 31−49.

[12] Zheng H, Zhang Y, Peng Z, *et al*. Influence of clay modification on the structure and mechanical properties of EPDM/montmorillonite nanocomposites. *Polym. Test.*, 2004, **23(2):** 217−223.

[13] Zhu J, Morgan A B, Lamelas F J, *et al*. Fire properties of polystyrene–clay nanocomposites. *Chem. Mater.*, 2001, **13(10):** 3774−3780.

[14] Gilman J W, Jackson C L, Morgan A B, *et al*. Flammability properties of polymer-layered silicate nanocomposites, propylene and polystyrene nanocomposites. *Chem. Mater.*, 2000, **12(7):** 1866−1873.

[15] Yano K, Usuki A, Okada A, *et al*. Synthesis and properties of polyimide–clay hybrid. *J. Polym. Sci., Part A: Polym. Chem.*, 1993, **31(10):** 2493−2498.

[16] Sinha R S, Yamada K, Okamoto M, *et al*. New polylactide/layered silicate nanocomposites. 3. High performance biodegradable materials. *Chem. Mater.*, 2003, **15(7):** 1456−1465.

[17] Nielsen L E. Models for the permeability of filled polymer systems. *J. Macromol. Sci. Chem.*, 1967, **1(5):** 929−942.

[18] He H, Frost R L, Bostrom T, *et al*. Changes in the morphology of organoclays with $HDTMA^+$ surfactant loading. *Appl. Clay Sci.*, 2006, **31(3/4):** 262−271.

[19] Denecke M A. Actinide speciation using X-ray absorption fine structure spectroscopy. *Coord. Chem. Rev.*, 2006, **250(7/8):** 730−754.

[20] Liu B, Wang X, Yang B, *et al*. Rapid modification of montmorillonite with novel cationic Gemini surfactants and its adsorption for methyl orange. *Mater. Chem. Phys.*, 2011, **130(3):** 1220−1226.

[21] Zhao F, Wan C, Bao X, *et al*. Modification of montmorillonite with aminopropylisooctyl polyhedral oligomeric silsequioxane. *J. Colloid Interface Sci.*, 2009, **333(1):** 164−170.

[22] Yui T, Yoshida H, Tachibana H, *et al*. Intercalation of polyfluorinated surfactants into clay minerals and the characterization of the hybrid compounds. *Langmuir*, 2002, **18(3):** 891−896.

[23] Harris D J, Bonagamba T J, Schmidt-Rohr K. Conformation of poly(ethylene oxide) intercalated in clay and MoS_2 studied by two-dimensional double-quantum NMR. *Macromolecules*, 1999, **32(20):** 6718−6724.

阳离子表面活性剂对钠基蒙脱土的插层改性研究

刘华斌, 肖汉宁

(湖南大学 材料科学与工程学院, 长沙 410082)

摘 要: 用十八烷基三甲基氯化铵(OTAC)通过离子交换法对钠基蒙脱土成功进行了有机化插层改性. 红外分析结果表明: OTAC 与蒙脱土之间发生了反应, X 射线衍射(XRD)分析结果显示随 OTAC 浓度的提高, 蒙脱土的(001)晶面间距逐渐扩大, 最大值可增至 3.80 nm; 基于以上分析研究, 假定了 OTAC 分子在蒙脱土片层间的排列分布状态. 扫描电镜(SEM)观察到改性前后蒙脱土的表面形貌发生了显著变化, 改性前蒙脱土团聚成大小不一的致密堆积颗粒, 而改性后的蒙脱土被剥离为松散的鱼鳞片状; 接触角测试和沉降实验结果表明, 改性后钠基蒙脱土的表面润湿性由亲水性转变为亲油性.

关 键 词: 蒙脱石; 插层改性; 微结构; 表面性能; 纳米材料

中图分类号: TQ174 **文献标识码:** A